eSim 2018
«BUILDING SIMULATION TO SUPPORT BUILDING SUSTAINABILITY»
IBPSA Canada
The Canadian Chapter of the International Building Performance Simulation Association
Le chapitre canadien de International Building Performance Simulation Association

Representation of daily profiles of building energy flexibility

Thibault Q. Péan[1,2], Bismark Torres[3], Jaume Salom[1], Joana Ortiz[1,2]

[1] IREC Catalonia Institute for Energy Research, Sant Adriá de Besós (Barcelona), Spain
[2] UPC Universitat Politècnica de Catalunya, Barcelona, Spain
[3] Universidad de Guayaquil, Guayaquil, Ecuador

Abstract: *The representation of simulation results with regards to building energy flexibility is investigated. The chosen case study is a residential flat located in Spain, equipped with an air-to-water heat pump. From a reference simulation scenario, active demand response (ADR) events are implemented; they consist in modulating the heating set-point for a few hours. If the starting time of the ADR event is varied in time, the resulting simulations enable to produce daily profiles quantifying the different aspects of energy flexibility. Different representations of these profiles are proposed and discussed, combining the flexibility capacity and efficiency profiles, or representing different ADR configurations in a single graph. A high dependency of the flexibility profiles was observed with regards to the existing consumption profile and temperature setbacks. An ADR event of 2 hours with set-point modulation of ±1°C provides a maximum flexibility capacity of 9.4kWh upwards and -8.6kWh downwards.*

Keywords: *energy flexibility in buildings, demand-side management, heat pump, flexibility representation.*

INTRODUCTION

Renewable energy sources (RES) constitute key elements in the global fight against climate change, as empowered notably by the 2015 Paris Agreement (UNFCC Conference of the Parties (COP) 2015) or the Sustainable Development Goals of the United Nations (United Nations General Assembly 2015). Variable RES such as wind and solar power, which production depends on the climatic conditions, represent a challenge for the management and stability of the power grids. Given that the price of solar and wind energy per kWh is becoming competitive against traditional fossil fuels (World Economic Forum 2016), such power plants are being installed at a high pace and thus innovative solutions will soon be needed to ensure a continuous and stable supply of electricity in the future.

Energy flexibility and demand-side management have long been identified as a potential to help solve these issues. In particular, the existing stock of buildings and their embedded thermal mass can be considered as possible energy storage which could help absorb the fluctuations caused by variable RES. The International Energy Agency – Energy in Buildings and Communities have gathered the investigations on this topic in its Annex 67 (Jensen et al. 2017). Within and also outside the framework of this project, extensive research has been carried out to try and define Key Performance Indicators (KPIs) for energy flexible buildings (Oldewurtel et al. 2013, De Coninck and Helsen 2016, Clauß et al. 2017, Reynders et al. 2017). These indicators generally take into account the dimensions of power, energy, time and cost inherent to flexibility (Lu and Hasan 2016). A first group of indicators intend to predict the available flexibility a priori (Reynders 2017). They can take the form of building time constants (Kensby et al. 2015), maximum time during which HVAC equipment can be turned on or off, power increase or decrease that can be maintained during a certain time (Six et al. 2011). Another group of indicators focus on an evaluation a posteriori of the flexibility performance resulting from certain implemented actions. These can for example take the form of cost/energy savings (Péan et al. 2017), load shifting and grid interaction indicators (Salom et al. 2014, Le Dréau and Heiselberg 2016), mostly in comparison with a reference case where no flexibility actions were implemented.

However there is no clear consensus on how these results could be represented graphically for a building, for example in the form of a daily flexibility profile. This remark is especially relevant since the flexibility (and consequently most of the associated KPIs) also depend on time. Such graphical content could be useful for several types of end-users: aggregators, utilities, electrical or mechanical engineers, designers. A standard representation could help them evaluate at a glance the available flexibility that a building can offer and at what cost, along the next day.

The present paper thus intends to perform an energy flexibility analysis on a test case, and proposes an example of representation of a daily profile showing both the capacity and the efficiency of energy flexibility. The focus thus lies more on how to represent the results than on the actual values of the flexibility (for this reason, only one sample day was used for testing the proposed approach). Applying the methods to a concrete case enabled to already

ISBN 978-2-921145-88-6

identify some practical issues in the implementation of the flexibility evaluation, which is already a valuable output of this research. The paper is structured as follows: in the 'Methods' section, the building study case is presented, as well as the simulation process implemented for the flexibility analysis, and a reminder of the KPIs utilized. In the 'Results' section, an example of time series is detailed, before the presentation of a daily profile showing the flexibility indicators for this specific building in different scenarios. Finally, discussions and conclusions are drawn.

METHODS

Building study case

Figure 1: Photograph of the studied building (the flat is on the first floor).

The building used as test case in this study is a flat of 109 m^2 located on the 1st floor of a multi-storey building. It is situated in the city of Terrassa and is representative of the construction habits of the region of Catalonia (Spain), especially for the period 1991-2007. In the present study, a refurbishment is considered with an additional 15 cm of insulation in the external walls, bringing their U-value down to 0.2 W/m^2·K. The dwelling is occupied by a family of four people (two adults and two children); their presence is modelled through a deterministic profile. The heating system consists of a circuit of eight radiators supplied by an air-to-water heat pump and controlled by a single thermostat placed in the living room. The apartment was modelled in TRNSYS and calibrated with metered data. More details about the assumptions can be found in the referenced articles (Ortiz et al. 2014, 2016, Péan et al. 2017). A time step of 3 minutes is utilized in the TRNSYS simulations.

Control strategy and ADR events

The flexibility potential is evaluated through dynamic building simulation, and the realization of so-called ADR events (Active Demand Response). The temperature set-point T_{SP} in the dwelling is normally set to $T_{ref} = 21.5$°C when the dayzone is occupied, and 20.5°C otherwise (i.e. at night or when the occupants are absent). An ADR event consists in deviating from this reference, by increasing/decreasing the set-point by $\pm\Delta T_{SP}$ during a period of l_{ADR}. The principle of this set-point modulation is presented in Figure 2 and can be summarized by the equation $T_{SP} = T_{ref} + \Delta T_{SP}$. The ADR event can be characterized by the different parameters T_{ref}, ΔT_{SP} and l_{ADR}. The different studied combinations of these parameters are summarized in Table 1. To characterize one case, a different simulation is carried out for every hour of the day: in each simulation, the ADR event starts at that hour. It is considered that only one ADR event can happen per day (therefore we discard the influence of successive events on each other).

The method is partly inspired from (Reynders et al. 2017). The main difference resides in the fact that the reference set-point T_{ref} is not the lower boundary of the comfort range, but its middle point. By placing the reference temperature at the middle of the comfort range, both

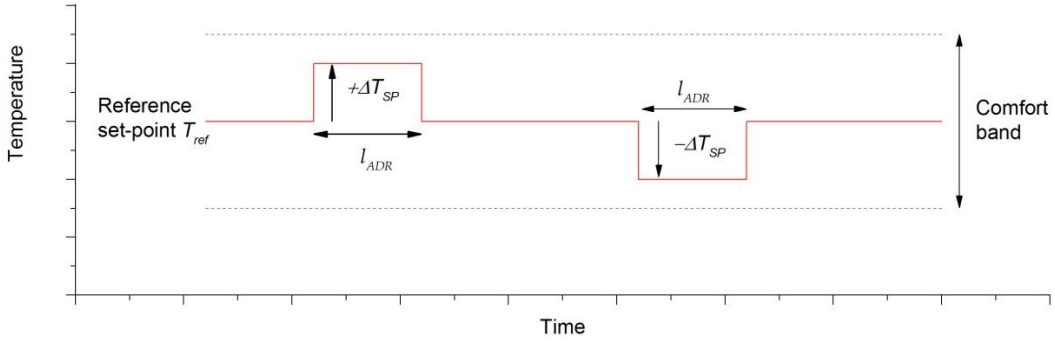

Figure 2: Conceptual principle of the set-point modulation. The resulting set-point is formed by the red line, parameterized by T_{ref}, ΔT_{SP} and l_{ADR}. Depending on the value of ΔT_{SP}, the set-point might exceed the comfort band boundaries at times.

ISBN 978-2-921145-88-6

upwards and downwards modulations are possible (while only upwards modulations are possible if the minimum comfort is considered).

Table 1: List of studied cases.

Case study	T_{SP} (occupied)	T_{SP} (night + unoccupied)	ΔT_{SP}	l_{ADR}
Reference	21.5°C	20.5°C	-	-
1D1H	21.5°C	20.5°C	± 1°C	1 h
1D2H	21.5°C	20.5°C	± 1°C	2 h
2D2H	21.5°C	20.5°C	± 2°C	2 h
1D5H	21.5°C	20.5°C	± 1°C	5 h

Performance indicators

The performance indicators used in this study are presented hereafter. More details about them can be found in (Reynders et al. 2017). The first indicator C_{ADR} represents the available storage capacity during the ADR event, and is calculated with (1). It corresponds to the deviation in energy of the ADR case compared to the reference case. In the integrals, Q_{ADR} and Q_{Ref} are respectively the thermal heating powers[1] of the ADR case and the reference case. It should be noted that here and contrary to (Reynders et al. 2017), Q_{Ref} does not correspond to the case which minimizes the heating energy, but rather a case with average set-point temperature in the middle of the comfort range. In this way, both upwards and downwards modulation can be studied.

In the case of an upwards modulation, C_{ADR} is positive and represents the additional energy stored within the building mass during l_{ADR}. In the case of a downwards modulation, C_{ADR} is negative and represents the energy "saved" compared to the reference case, during l_{ADR}.

$$C_{ADR} = \int_0^{l_{ADR}} (Q_{ADR} - Q_{Ref})\, dt \qquad (1)$$

Charging/discharging energy within the building thermal mass comes at a certain cost, due to the extra losses caused by this operation. In order to take into account the effect of these losses, a storage efficiency[2] is defined, as shown in (2):

$$\eta_{ADR} = 1 - \frac{\int_0^{\infty} (Q_{ADR} - Q_{Ref})dt}{\left|\int_0^{l_{ADR}} (Q_{ADR} - Q_{Ref})dt\right|} \qquad (2)$$

In the case of an upwards modulation, (2) can be interpreted as follows:

$$\eta_{ADR} = 1 - \frac{energy\ losses}{stored\ energy} \qquad (3)$$

By reorganizing this equation, the storage efficiency can alternatively be interpreted as the ratio between the "rebound effect" and the "ADR event", as shown in (4). In the case of an upwards modulation, this corresponds to the ratio between the energy saved after the ADR event and the surplus energy stored during the ADR event. In the case of a downwards modulation, it corresponds to the ratio between the surplus energy spent in the period after the ADR event and the energy saved during the ADR event.

$$\eta_{ADR} = \frac{\int_{l_{ADR}}^{\infty} (Q_{ADR} - Q_{Ref})dt}{\left|\int_0^{l_{ADR}} (Q_{ADR} - Q_{Ref})dt\right|} = \frac{"rebound"}{"ADR\ event"} \qquad (4)$$

The integrals used in the calculation of η_{ADR} are theoretically summed over an infinite period of time. In the present study, only the 24 hours ahead from the start of the ADR event have been considered. It is assumed that the ADR event has little to no effect on the behavior of the system after this limit in the present studied case.

RESULTS

Analysis of one example of an ADR event

An example of ADR event is shown in Figure 3. In the present case (1D2H), it consists of a downwards set-point modulation: at 6:00, the heating set-point is reduced of 1°C, for the subsequent period of 2 hours (grey area), as can be seen on the dashed lines of the top graph. It can be observed on the bottom graph that the heating system is thus stopped during all the ADR event. Consequently, it needs to operate during longer and more frequent periods right after the ADR event (approximately from 8:00 to 17:00). The heat that has not been supplied during the ADR event has to be provided in the following hours. From 17:00, the system goes back to operating in a very similar way than the reference case, despite a small shifting due to differences in the prior evolution. The indicator C_{ADR} can be represented graphically by the area under the power shifting curve during the ADR event. A similar analysis could be made for the corresponding upwards modulation.

[1] This was chosen to have a result independent of the heating system. To get an insight more directly relevant for the grid side, the electrical power of the heat pump could be used instead in the same formulas.

[2] An absolute value was added in the denominator: in this way, the efficiency is higher than 1 if the overall energy use is lower than in the reference case, both with upwards and downwards modulations.

ISBN 978-2-921145-88-6

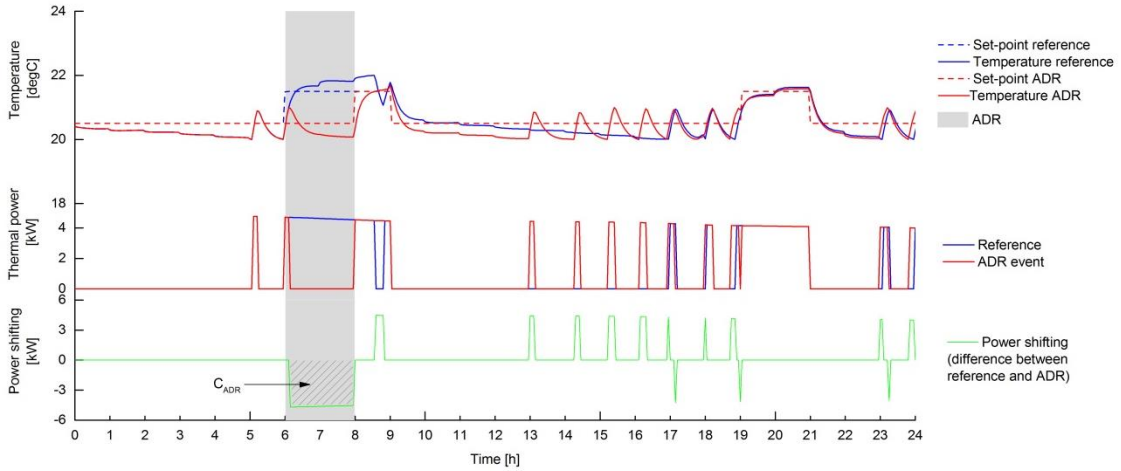

Figure 3: Time series (24 hours) of the reference scenario (in blue), compared to the scenario where a downwards ADR event takes place at 6:00 (1D2H, in red). The indoor temperature is shown in the top graph, the thermal heating power in the middle graph and the power shifting in the bottom graph.

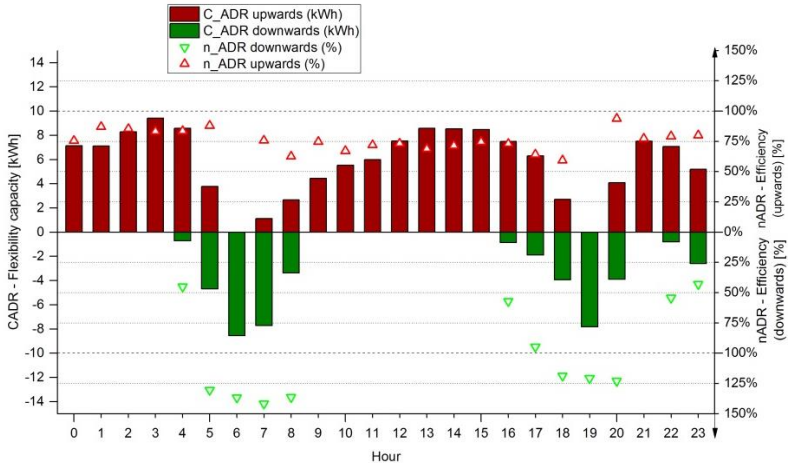

Figure 4: Daily profile of the indicators C_{ADR} and η_{ADR}, with an ADR of 2 hours, and a modulation of ±1°C. The graph should be read symmetrically with regards to the zero horizontal axis: C_{ADR} and η_{ADR} are represented in red in the upper part of the graph for the upwards modulation; and in green in the bottom part of the graph for the downwards modulation.

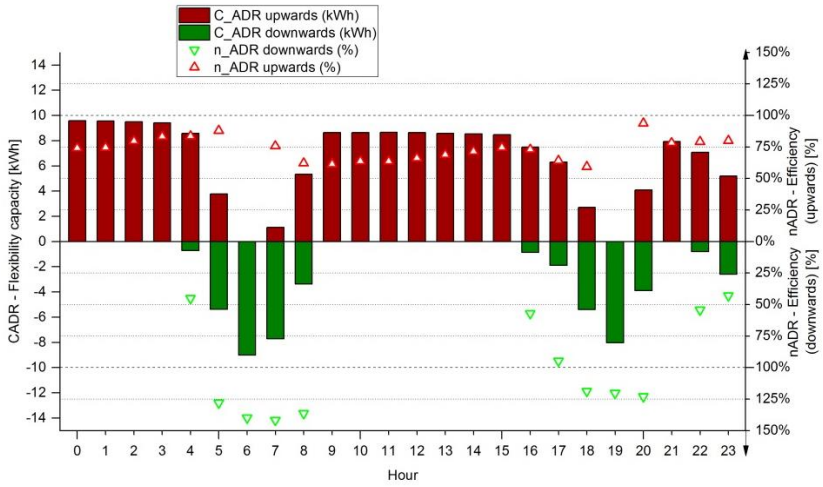

Figure 5: Daily profile of the indicators C_{ADR} and η_{ADR}, with an ADR of 2 hours, and a modulation of ±2°C.

ISBN 978-2-921145-88-6

Representation of C_{ADR} and η_{ADR}: case 1D2H

The simulation and the analysis is repeated for the ADR event taking place at every hour of the day (from hour 0 to hour 23), to observe the eventual differences in flexibility capacity and efficiency at different times. The chosen test day is the 30th of January, considered as representative of a cold winter day in Spain. The weather conditions for that day can be observed in Figure 6. For a full flexibility analysis, other test days in shoulder season could also be studied. However, since the present work focuses more on the representation rather than on the complete flexibility evaluation, only one winter day was considered.

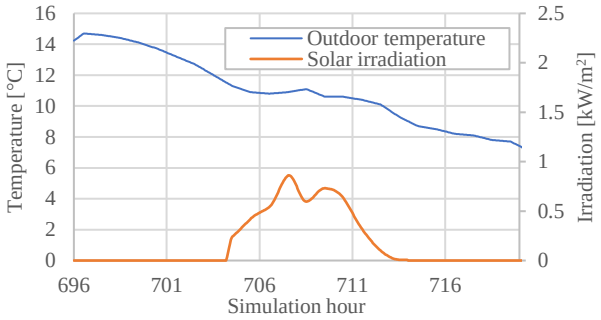

Figure 6: Weather conditions during the tested day.

The indicators are computed for every simulation realized, which leads to the graph presented in Figure 4. In red are represented the results of the upwards modulations, and in green, the results of the downwards modulations; the bars represent the capacity C_{ADR} while the symbols represent the efficiency η_{ADR}. It should be noted that for the downwards case, the efficiency is plotted reversely, so as to obtain a symmetrical graph with regards to the zero horizontal axis (see the vertical axis on the right). When $C_{ADR} = 0$, η_{ADR} is not computed since an efficiency is meaningless when there is no actual capacity for flexibility.

The shape of the daily profile presented in Figure 4 corresponds to the expectations, considering the occupancy profile. During the peak hours (~5:00 to 8:00 and 18:00 to 20:00), the occupants are present in the building, and the set-point is thus already increased. Therefore, the heat pump is generally switched on already in the reference case. Increasing the set-point at these moments does not allow for supplementary upwards flexibility ($C_{ADR} = 0$ at 6:00 and 19:00). However, a downwards flexibility is logically available if the set-point is reduced during these hours: up to 8.5 kWh can be saved during the 2 hours of the ADR event (at 6:00 in the morning).

Conversely, the system presents the opposite behavior during non-occupied and night hours, mainly from 0:00 to 4:00 and from 9:00 to 15:00. In these periods, the setback provokes a switching off of the heat pump already in the reference scenario. The only available flexibility thus consists in forcing the heat pump to operate, by raising the set-point. In this way, a maximum of $C_{ADR} = 9.4\ kWh$ can be reached during the 2 hours ADR event (maximum reached at 3:00).

The analysis of η_{ADR} shows some discrepancies between the upwards and the downwards modulation cases. The efficiency ranges from 59 to 94% in the upwards case, and is relatively stable. In the downwards cases, and more specifically those with a high capacity C_{ADR}, the efficiency reaches levels above 100%, up to 123%. Concretely, this means that the system saves energy that was not necessary to use in the first place: the energy saved during the ADR event is not compensated entirely by a posterior use of energy (rebound effect is thus limited). This operation causes obviously a slight decrease in the temperature, but since the reference case was not the case of minimum comfort, some margin still exists until the bottom comfort boundary is reached, and thus the comfort requirements are still met.

Representation of C_{ADR} and η_{ADR}: case 2D2H

The same analysis is carried out with the case 2D2H, hence with an amplitude of the set-point modulation of 2°C, instead of 1°C in the previous case. The results are presented in Figure 5, with the same layout than Figure 4. The daily profile appears similar to the previous case. At some hours, the supplementary ±1°C enables to provide more flexibility capacity, but an upper limit is observed around 9.5 kWh. This saturation corresponds to the operation (or complete stop) of the heat pump during the entire ADR event, therefore increasing (or decreasing) the set-point more does not permit to increase the flexibility capacity further.

Figure 5 can be compared with the results presented in (Reynders et al. 2017). In this reference, the authors have analyzed a similar case (2D2H), for residential buildings in Belgium. The authors only studied the upwards flexibility and represented the daily profile of C_{ADR} as an average of several days. However the daily profile of C_{ADR} showed a very similar shape. One notable difference consists in the two valleys of the profile (at 6:00 and 19:00): in (Reynders et al. 2017), these two lower valleys are visible but an upwards flexibility is still available. In Figure 5, $C_{ADR} = 0\ kWh$ at these hours, hence no upwards flexibility is possible (because the set-point is already increased in the reference case at these hours). This difference could be due to the fact that the reference temperature T_{ref} was chosen at the lower limit of the comfort range in (Reynders et al. 2017), hence always keeping a possibility for upwards modulation.

ISBN 978-2-921145-88-6

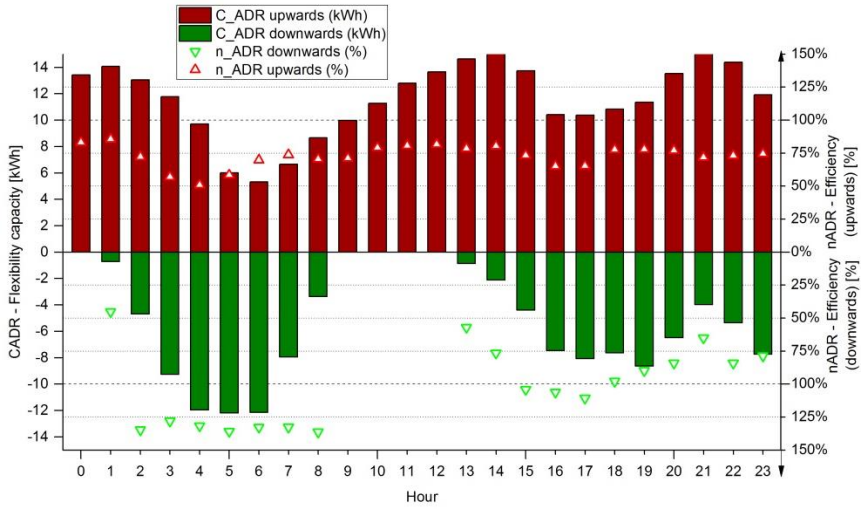

Figure 7: Daily profile of the indicators C_{ADR} and η_{ADR}, with an ADR of 5 hours, and a modulation of ±1°C

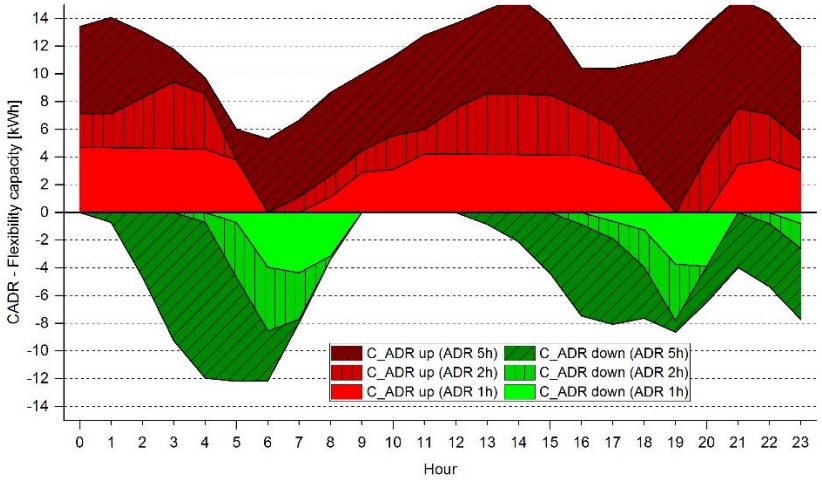

Figure 8: Representation of the daily profile of C_{ADR} for different durations of the ADR event.

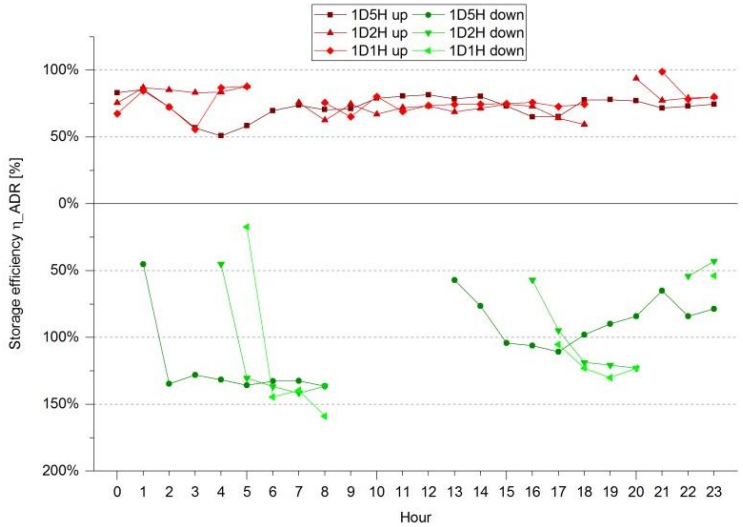

Figure 9: Representation of the daily profile of η_{ADR} for different durations of the ADR event.

ISBN 978-2-921145-88-6

Representation of C_{ADR} and η_{ADR}: case 1D5H

Case 1D5H is represented in Figure 7, with ADR events lasting for 5 hours instead of 2 hours in the two previous cases. With this lengthened duration, the potential for energy flexibility clearly increases, since more time is available for operating the heat pump and storing thermal energy. The efficiency of the load shifting however decreases, due to the prolonged storage operation and hence higher thermal losses. For example at hour 3, the upwards capacity is increased from 9.4 kWh to 11.7 kWh while the efficiency dropped from 83% to 57%. Increasing the duration of the ADR event thus does not necessarily present interest.

Alternative representation of C_{ADR}, with ADR events of different durations

An alternative graphical representation of the daily C_{ADR} profile is proposed in Figure 8, comparing different durations of the ADR event, keeping the same amplitude of the temperature variation (±1°C). In red, the upwards modulation is shown, and in green the downwards modulation. From lighter to darker color indicates a longer duration of the ADR event: 1h, 2h and 5h. With a longer ADR, the flexibility capacity obviously increases, and with a 5h event, there is a potential for flexibility all day long (while some hours presented little to no flexibility with an ADR event of only 1 or 2h).

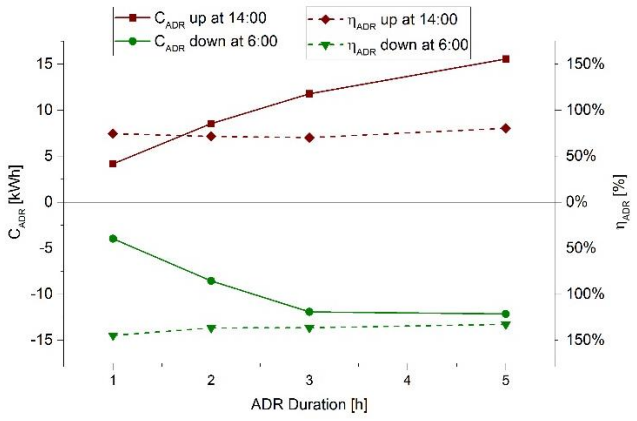

Figure 10: Flexibility capacity at selected hours, in function of the length of the ADR event.

The interest of this representation is to show at a glance the comparison between different configurations of the ADR event. It does however not reveal the drop of efficiency due to the longer ADR events, which should be taken into account when actually using the flexibility. For this reason, the efficiency profiles have been plotted on Figure 9. The efficiency drop due to longer ADR events (1D5H) is visible especially in the early morning hours for the upwards flexibility events and in the evening for the downwards flexibility events.

Since the maximum upwards flexibility almost always occur at 14:00 and the maximum downwards flexibility occur at 6:00, these hours of the day can be isolated to be plotted on a single graph, as shown in Figure 10. A saturation occurs for ADR events of 5 hours, especially for the downwards modulation case. It is therefore concluded that events of 3 hours provide sufficient flexibility and increasing the ADR duration to 5 hours do not provide supplementary benefits in the studied case. Furthermore, the efficiency remains almost constant in this case.

Alternative representations in relation with the reference consumption profile

Another suggestion for representation consists in additionally plotting the reference energy consumption, as shown in Figure 11 (black solid line). This enables to put in relation the actual energy consumption with the flexibility potential. From the black line representing the load, the additional upwards flexibility is shown as a red area above the line, and the downwards flexibility is shown as a green area below the line. It can be seen that the periods of high energy consumption logically correspond to a downwards flexibility potential, while the periods with no consumption corresponds to upwards flexibility potential. This graph however does not provide information on the efficiency of the ADR event, therefore it should be complemented with another graph representing this aspect, so as to obtain a global overview of the flexibility potential.

Figure 11 represents the flexibility available for events of 1 hour durations. It can be argued that this is the most relevant information for aggregation at an upper level, since the regulation and balancing markets operate on a 24 hours horizon with a time resolution of 1 hour (Marszal-Pomianowska et al. 2017)

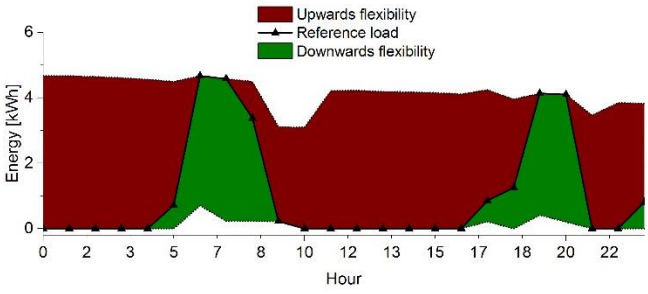

Figure 11: Representation of the flexibility potential (upwards and downwards) starting from the reference energy consumption profile. Case 1D1H.

ISBN 978-2-921145-88-6

ADR events of 2 hours duration can also be represented in a similar manner. In this case, the reference load profile should be as well aggregated per clusters of 2 hours, to enable an easier comparison. An example is presented in Figure 12. Furthermore, events of different modulation amplitude are plotted in this graph: the flexibility capacity of a set-point modulation of ±1°C is shown in light green and red, while the modulation of ±2°C is shown in dark green and red. In this way, the additional benefits of amplifying the set-point modulation are revealed. It can be seen for example that further increasing the set-point provides greater upwards flexibility only in the early hours of the day (0:00 to 2:00) and after the morning occupancy (8:00 to 12:00). Further decreasing the set-point usually does not provide greater downwards flexibility, except at 18:00.

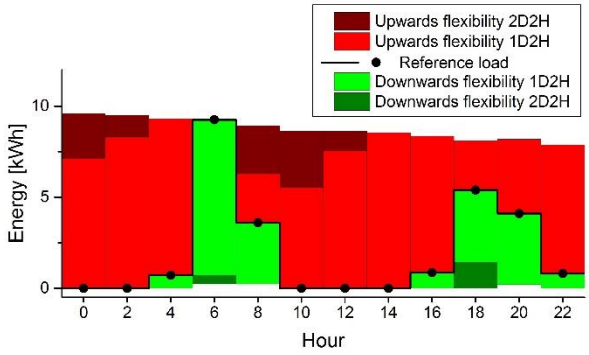

Figure 12: Representation of the flexibility potential (upwards and downwards) starting from the reference energy consumption profile, aggregated per periods of 2 hours. Cases 1D2H and 2D2H.

DISCUSSIONS

Firstly, the present study constituted an interesting example of applying the calculation methods of flexibility KPIs to a real study case. This process revealed some relevant aspects. For instance, interpreting the results of the storage efficiency required some adaptations in the downwards flexibility case, by integrating an absolute value in the formula. Moreover, the integrals in the formula of η_{ADR} are theoretically computed until ∞. In the present case, it was chosen to calculate them for 24 hours ahead since it is assumed that the ADR event will have little effect after these 24 hours and the system will already be back to normal (reference) operation. However, a little shifting of the energy use is observed. Due to the nature of the ON/OFF system, this provokes the "symmetrical spike" pattern observed for example the bottom graph of Figure 3 at 17:00. It should be noted that if the end of the integral falls just between these two spikes, the result of the efficiency calculation could be distorted by this effect. The application of the storage efficiency calculation should therefore be realized with care.

The present work also revealed some limits of the considered KPIs. Firstly, C_{ADR} and η_{ADR} consider the flexibility in terms of thermal heating power delivered by the emitter to the building. The advantage of such concept resides in the fact that the results are independent from the heating system installed in the building. However, it could be more interesting to consider the electrical power flexibility (after applying the efficiencies and coefficients of performance of the system), so that the grid side can know what available power flexibility it can retrieve from a building. Furthermore, the flexibility capacity (energy, in kWh) available during the ADR event does not guarantee that this flexibility will be provided evenly during the duration of the ADR event (i.e. at a constant power). The accuracy and interest of this flexibility forecast might therefore be limited. It would still be useful at a higher aggregated level, where the individual behavior of each building matters less, provided that they can supply the required amount of energy flexibility during a fixed period. Another disadvantage of the applied method is that it only considers one ADR event during the day. In real applications, a building could probably be activated for DSM several times during a day, and then the 24 hours flexibility forecast is no longer valid after the first ADR event. This aspect could be studied in further research.

From the represented graphs, it can be deduced that the existing occupancy schedule has a crucial influence on the flexibility potential: it actually shapes the daily profile of energy flexibility. Roughly, the occupancy periods (with already increased energy consumption) correspond to downwards flexibility potential, while the periods of unoccupancy or night correspond to upwards flexibility potential. Considering a flat temperature set-point of reference or a different occupancy schedule would considerably change the flexibility evaluation.

Many discussions already arose within the IEA EBC Annex 67 about the choice and impact of a reference case when computing a building's energy flexibility. In the present work, the reference case was chosen with a set-point at the middle of the comfort range (and not the lower boundary like in (Reynders et al. 2017)). In this way, both the upwards and downwards flexibility can be calculated. Furthermore, it gives a more realistic idea of the flexibility potential of the dwelling. Considering the minimum energy use as reference would on the other hand enable to calculate the highest flexibility potential, but most probably not all this potential could be harvested in a real operational case.

ISBN 978-2-921145-88-6

CONCLUSIONS

In the present study, indicators for energy flexibility were computed for the case of a residential dwelling in the Mediterranean climate zone. Different representations of these indicators in the form of daily profiles were proposed. The first graph type (Figure 4, Figure 5 and Figure 7) enables to show graphically both the flexibility energy capacity and its storage efficiency along the day, and for both upwards and downwards flexibility. This representation thus gives a good overview of the different aspects of energy flexibility for a building in a single graph. When comparing different configurations of the ADR event, the area graph (Figure 8) seems a better option for the flexibility capacity, but then the efficiency profiles should be plotted apart.

In all representations, it was found that this profile highly depends on temperature setbacks existing in the reference scenario. A set-point modulation of ±1°C during 2 hours enables to provide a maximum of 9.4 kWh in available flexibility capacity (upwards), and -8.6 kWh (downwards). Lengthening the duration of this ADR event enables to increase the capacity, but saturation is observed and the storage efficiency then tends to decrease.

A single winter day was utilized to evaluate the flexibility in this study case. To fully characterize the flexibility potential represented by this dwelling, a similar study should be carried out for several test days covering the whole heating season, hence including also days in Spring where the heating needs are lower. Furthermore, it would also be interesting to apply the calculations of the indicators and the graphical representation to cases of cooling, where the flexibility would be reversed in terms of heat storage.

ACKNOWLEDGEMENTS

This project has received funding from the European Union's Horizon 2020 research and innovation programme under the Marie Skłodowska-Curie grant agreement No 675318 (INCITE). Part of this work stems from the activities carried out in the framework of the IEA-EBC Annex 67 (International Energy Agency – Energy in Buildings and Communities program) about Energy Flexibility in Buildings.

REFERENCES

Clauß, J., P. Vogler-Finck, C. J. Finck, and P. Beagon. 2017. Control Strategies for Building Energy Systems to Unlock Demand Side Flexibility - A Review. Page *Building Simulation*. San Francisco, USA.

De Coninck, R., and L. Helsen. 2016. Quantification of flexibility in buildings by cost curves - Methodology and application. *Applied Energy* 162:653–665.

Le Dréau, J., and P. Heiselberg. 2016. Energy flexibility of residential buildings using short term heat storage in the thermal mass. *Energy* 111(1):1–5.

Jensen, S. Ø., A. Marszal-Pomianowska, R. Lollini, W. Pasut, A. Knotzer, P. Engelmann, A. Stafford, and G. Reynders. 2017. IEA EBC Annex 67 Energy Flexible Buildings. *Energy and Buildings* 155:25–34.

Kensby, J., A. Trüschel, and J.-O. Dalenbäck. 2015. Potential of residential buildings as thermal energy storage in district heating systems – Results from a pilot test. *Applied Energy* 137:773–781.

Lu, M., and A. Hasan. 2016. Literature Review on Metrics and Indicators for Energy Flexibility in Single Buildings, Internal Report - IEA EBC Annex 67 Activity A.2.1.

Marszal-Pomianowska, A., J. Stoustrup, J. Widén, and J. Le Dréau. 2017. Simple flexibility factor to facilitate the design of energy-flex-buildings. Pages 1205–121*215th International Conference of the International Building Performance Simulation Association (IBPSA)*. San Francisco, USA.

Oldewurtel, F., D. Sturzenegger, G. Andersson, M. Morari, and R. S. Smith. 2013. Towards a standardized building assessment for demand response. *Proceedings of the IEEE Conference on Decision and Control*:7083–7088.

Ortiz, J., A. Fonseca, J. Salom, N. Garrido, P. Fonseca, and V. Russo. 2016. Comfort and economic criteria for selecting passive measures for the energy refurbishment of residential buildings in Catalonia. *Energy and Buildings* 110:195–210.

Ortiz, J., F. Guarino, J. Salom, C. Corchero, and M. Cellura. 2014. Stochastic model for electrical loads in Mediterranean residential buildings: Validation and applications. *Energy and Buildings* 80:23–36.

Péan, T., J. Ortiz, and J. Salom. 2017. Impact of Demand-Side Management on Thermal Comfort and Energy Costs in a Residential nZEB. *Buildings* 7(2):37.

Reynders, G. 2017. IEA EBC Annex 67 Common Exercise session - Internal communications of the 4th Annex 67 meeting. Freiburg, Germany.

Reynders, G., J. Diriken, and D. Saelens. 2017. Generic characterization method for energy flexibility: Applied to structural thermal storage in residential buildings. *Applied Energy* 198:192–202.

Salom, J., A. J. Marszal, J. Widén, J. Candanedo, and K. B. Lindberg. 2014. Analysis of load match and grid interaction indicators in net zero energy buildings with simulated and monitored data. *Applied Energy* 136:119–131.

Six, D., J. Desmedt, J. V. A. N. Bael, and D. Vanhoudt.

ISBN 978-2-921145-88-6

2011. Exploring the Flexibility Potential of Residential Heat Pumps. *21st International Conference on Electricity Distribution*(442):6–9.

UNFCC Conference of the Parties (COP). 2015. Adoption of the Paris Agreement. Proposal by the President. Page FCCC/CP/2015/L.9/Rev.1. FCCC/CP/2015/L.9/Rev.1, Geneva (Switzerland).

United Nations General Assembly. 2015. Transforming our world: The 2030 agenda for sustainable development. *https://sustainabledevelopment.un.org/content/documents/7891Transforming%20Our%20World.pdf*(1):1–5.

World Economic Forum. 2016. Renewable Infrastructure Investment Handbook: A Guide for Institutional Investors(December):43.

ISBN 978-2-921145-88-6